




”

Article

Discrete Vacuum Geometry Predicts the Hierarchical Mass Spectrum of Standard Model Fermions

Yuxuan Zhang ^{1,*} , Weitong Hu ²  and Wei Zhang ³ 

¹ College of Communication Engineering, Jilin University, Changchun 130012, China; csoft@live.cn

² Aviation University of Air Force, Changchun 130022, China

³ College of Computer Science and Technology, Jilin University, Changchun 130012, China; zwei25@mails.jlu.edu.cn

* Correspondence: csoft@live.cn

Abstract

The fermion mass hierarchy in the Standard Model spans six chief orders of magnitude and is conventionally explained by arbitrary Yukawa couplings. Here we explore a purely mathematical construction—a discrete vacuum geometry derived from a finite-dimensional 19D $(12+4+3)$ \mathbb{Z}_3 -graded Lie superalgebra with exact triality symmetry—and examine whether simple integer lattice vectors embedded in its extended \mathbb{Z}^3 lattice happen to produce mass ratios and other parameter values resembling those observed in nature. Using a geometric scaling $m \propto L^{-2}$ where L is the Euclidean norm of selected lattice vectors, and anchoring to the top-quark mass (173 GeV), the framework yields the following curious numerical proximities: electron 0.49 MeV (4.6% agreement), muon 118 MeV (12%), qualitative up/down quark mass inversion $m_u < m_d$, exact Weinberg angle $\sin^2 \theta_W = 0.25$, a Higgs-related scale ratio of 0.727 (0.3%), strong/weak coupling ratio ≈ 0.95 (near equipartition), CKM CP phase $\approx 65.3^\circ$ (5%), and neutrino mixing angles of exactly 45° (maximal atmospheric) with $\cos^2 \theta_{12} = 1/3$ (exact tri-bimaximal solar angle). These alignments, along with geometric patterns resembling tri-bimaximal neutrino mixing, are presented as intriguing mathematical coincidences within an abstract algebraic framework and do not constitute evidence of physical relevance or predictive power. The construction offers a speculative geometric perspective that unifies gauge and flavor aspects in a single algebraic setting, extending previous work on the same structure, while emphasising that the observed numerical matches may reflect serendipity rather than deeper significance.

Keywords: \mathbb{Z}_3 -graded Lie superalgebras; discrete vacuum geometry; fermion mass ratios; geometric scaling; triality symmetry; integer lattice embedding; numerical coincidences; Standard Model parameters



Academic Editor: Firstname Lastname

Received: 22 November 2025

Revised: 24 December 2025

Accepted: 25 December 2025

Published:

Citation: . . . *Universe* **2026**, *10*, 0.

Copyright: © 2026 by the authors.

Licensee MDPI, Basel, Switzerland.

This article is an open access article distributed under the terms and conditions of the Creative Commons Attribution (CC BY) license

(<https://creativecommons.org/licenses/by/4.0/>).

1. Discrete Vacuum Geometry: Algebraic Foundation and Numerical Patterns in Fermion Masses

1.1. Introduction to the Framework

The Standard Model (SM) of particle physics, combined with General Relativity, accurately describes a broad range of natural phenomena, yet it depends on approximately 26 independent input parameters, including fermion masses, mixing angles, gauge couplings, and the cosmological constant. The fermion masses span six orders of magnitude, from the top quark ($m_t \approx 173$ GeV) to the electron ($m_e \approx 0.511$ MeV). Traditional explanations often introduce additional free parameters.

In this work, we explore a purely mathematical construction based on a discrete vacuum geometry rooted in a 19-dimensional \mathbb{Z}_3 -graded Lie superalgebra $\mathfrak{g} = \mathfrak{g}_0 \oplus \mathfrak{g}_1 \oplus \mathfrak{g}_2$ (dimensions 12+4+3) [1]. The grade-2 sector supports triality automorphisms, generating a finite 44-vector Core Lattice that yields the tree-level Weinberg angle $\sin^2 \theta_W = 0.25$ exactly. An infinite integer extension (\mathbb{Z}^3) of this lattice allows simple integer vectors whose Euclidean norms, via a formal geometric scaling $m \propto L^{-2}$ anchored to the top quark, happen to produce mass scales curiously close to several observed charged fermion masses.

Additional geometric patterns in the same lattice coincidentally resemble features of neutrino mixing angles and provide a combinatorial factor that numerically aligns with the observed scale of the cosmological constant. These alignments are presented as mathematical curiosities within an abstract algebraic framework and do not constitute physical predictions. The construction extends earlier work deriving $\sin^2 \theta_W = 0.25$ exactly from the same structure and offers a speculative geometric perspective on gauge and flavor parameters.

1.2. The Algebraic Foundation

The framework begins with a finite-dimensional \mathbb{Z}_3 -graded Lie superalgebra $\mathfrak{g} = \mathfrak{g}_0 \oplus \mathfrak{g}_1 \oplus \mathfrak{g}_2$ (dimensions 12+4+3), featuring:

- a triality automorphism τ of order 3 with $\tau^3 = \text{id}$,
- a unique (up to scale) invariant cubic form on the grade-2 sector \mathfrak{g}_2 ,
- graded brackets satisfying \mathbb{Z}_3 -generalized Jacobi identities, verified symbolically in critical sectors and numerically with residuals $\leq 8 \times 10^{-13}$ over 10^7 random tests in a faithful matrix representation.

The graded Jacobi identity takes the form:

$$[[X, Y], Z] + \omega^{\deg(X) \deg(Y)} [[Y, Z], X] + \omega^{\deg(Y) \deg(Z)} [[Z, X], Y] = 0,$$

where $\omega = e^{2\pi i/3}$. The cubic invariant on the 3-dimensional grade-2 sector drives the triality symmetry, enabling the spontaneous generation of a closed 44-vector core lattice under repeated triality operations.

1.3. The Two-Layer Vacuum Model

We consider a mathematical two-layer description of the vacuum structure derived from the algebra:

1. **The Core Lattice (finite, 44 vectors):** Generated by non-linear triality saturation starting from the democratic vacuum alignment fixed by the cubic invariant. This finite set defines a geometric ratio yielding $\sin^2 \theta_W = 0.25$ exactly.
2. **The Extended Lattice (\mathbb{Z}^3):** The infinite integer span of the core basis vectors. Simple sites in this lattice are examined for possible numerical relations to low-energy fermion scales.

1.4. Geometric Derivation of the Weinberg Angle

Repeated application of triality operations to the grade-2 vacuum sector spontaneously saturates at exactly 44 vectors. Classification by Euclidean length yields 11 vectors associated with the weak sector due to democratic alignment in the vacuum, giving the geometric ratio

$$\sin^2 \theta_W = \frac{11}{44} = 0.25 \quad (\text{exact match to tree-level GUT value}).$$

The observed low-energy value $\sin^2 \theta_W \approx 0.231$ is accounted for by standard renormalization-group evolution.

1.5. Geometric Scaling and Numerical Coincidences in the Fermion Mass Spectrum

In the extended \mathbb{Z}^3 lattice, we tentatively associate certain low-norm integer vectors with fermions and examine the scaling

$$m_f \approx M_0 / \|\mathbf{v}_f\|^2,$$

with M_0 anchored to the top quark mass ($L^2 = 1$). A computational search identifies vectors whose norms yield scales curiously close to several observed charged fermion masses (Table 1). Deviations, particularly for heavier quarks, are qualitatively consistent with expected QCD renormalization effects running from a high scale, though this interpretation remains speculative.

These numerical agreements are presented as intriguing mathematical coincidences and may reflect serendipity rather than physical significance. No mechanism is claimed to enforce the specific vector–fermion associations beyond the observed proximity.

Table 1. Numerical coincidences between lattice-derived scales (M_0 anchored to $m_t = 173$ GeV) and experimental pole masses. Agreements are mathematical only.

Particle	L^2	Example Vector	Derived (MeV)	Exp. (MeV)	Relative Deviation
Top	1	[0,0,1]	172,760	172,760	0%
Bottom	54	[1,2,7]	3,199	4,180	−23%
Charm	162	[0,9,9]	1,066	1,275	−16%
Tau	162	[0,9,9]	1,066	1,776	−40%
Muon	1458	[0,27,27]	118.5	105.7	+12%
Down	39366	[1,46,193]	4.39	4.70	−6.6%
Electron	354294	[3,138,579]	0.488	0.511	−4.6%

The electron agreement (4.6% across six orders of magnitude) and muon proximity are notable curiosities, while heavier quark deviations align qualitatively with known running effects. Additionally, the lattice ordering coincidentally suggests a qualitative up/down quark mass inversion ($m_u < m_d$).

1.6. Geometric Patterns in Flavor Mixing Angles

The same lattice structure yields additional geometric patterns that coincidentally resemble observed features of neutrino and quark mixing.

1.6.1. Physical Picture: Core Symmetry vs Hybrid Perturbations

In the lattice interpretation:

- Quark mixing (CKM): Dominated by hybrid vectors of the form $[-2, 1, 1]$ (two components equal, one opposite), reflecting strong anisotropy. Misalignments from the democratic vacuum $[1, 1, 1]$ are small, yielding hierarchical angles.
- Neutrino mixing (PMNS): Dominated by basis vectors $[1, 0, 0]$ and root vectors $[1, -1, 0]$ or $[0, 1, 1]$, reflecting higher symmetry for colorless leptons. The y- and z-axes are equivalent under triality, with bisector $[0, 1, 1]$ yielding maximal 45° mixing.

This geometric distinction coincidentally mirrors the observed "flavor puzzle" (large neutrino mixing vs small quark mixing).

The atmospheric angle corresponds to the angle between basis directions projected onto the symmetric root $[0, 1, 1]$:

$$\theta_{23} = 45^\circ, \quad \sin^2 \theta_{23} = 0.5 \quad (\text{maximal mixing}).$$

The solar angle relates to the magic angle between basis and democratic vectors ($\arccos(1/\sqrt{3}) \approx 54.7^\circ$), yielding $\cos^2 \theta_{12} = 1/3 \approx 0.333$ —exactly the tri-bimaximal (TBM) prediction.

1.6.2. Numerical Verification in the Lattice

The following simple computation illustrates these geometric values:

```
import numpy as np

print("=== Z3 Lattice: Neutrino PMNS Mixing Angles ===\n")

# Basis vectors (flavor eigenstates)
e1 = np.array([1, 0, 0])
e2 = np.array([0, 1, 0])
e3 = np.array([0, 0, 1])

# Symmetric root for atmospheric mixing
root_23 = np.array([0, 1, 1]); root_23 = root_23 / np.linalg.norm(
    root_23)

cos_23 = np.dot(e2, root_23)
theta_23 = np.degrees(np.arccos(cos_23))
sin_sq_23 = np.sin(np.radians(theta_23))**2

print(f"Angle(e2, [0,1,1]): {theta_23:.2f} deg")
print(f"sin^2(theta_23): {sin_sq_23:.4f}")
print(f"Geometry Prediction: 0.500 (Maximal Mixing)")

# Democratic vector for solar mixing
dem = np.array([1, 1, 1]); dem = dem / np.linalg.norm(dem)
cos_sol = np.dot(e1, dem)
theta_sol = np.degrees(np.arccos(cos_sol))
cos_sq_sol = cos_sol**2

print(f"\nAngle(e1, [1,1,1]): {theta_sol:.2f} deg (Magic Angle)")
print(f"cos^2(theta): {cos_sq_sol:.4f}")
print(f"Prediction: 0.3333 (1/3)")
print("[RESULT] Matches Tribimaximal Mixing (TBM) Ansatz exactly.")
```

Listing 1: Geometric Derivation of Neutrino Mixing Angles

Execution Results: - Atmospheric mixing: $\theta_{23} = 45.00^\circ$, $\sin^2 \theta_{23} = 0.5000$ (maximal; experimental $\sim 0.546 \pm 0.02$). - Solar mixing: Magic angle 54.74° , $\cos^2 \theta_{12} = 0.3333$ (exactly $1/3$, matching TBM prediction; experimental $\sin^2 \theta_{12} \approx 0.307$).

These exact geometric values coincidentally reproduce the tri-bimaximal ansatz for neutrino mixing. Small experimental deviations may reflect higher-order effects or be coincidental.

1.7. Geometric Perspective on the Cosmological Constant

The cosmological constant problem involves a vast discrepancy between naive QFT estimates ($\sim M_{\text{Pl}}^4$) and the observed value ($\Lambda_{\text{obs}} \sim 10^{-122} M_{\text{Pl}}^4$). The lattice structure offers a combinatorial calculation that yields an intriguing numerical coincidence.

1.7.1. Physical Picture: Geometric Seesaw and Combinatorial Enhancement

A graded seesaw mechanism yields an exponential suppression:

$$\Lambda \sim M_{\text{Pl}}^4 e^{-8\pi\kappa}, \quad (1)$$

where κ is a geometric factor from the lattice, producing $e^{-8\pi\kappa} \sim 10^{-128}$. This strong suppression overcompensates the observed value by $\sim 10^{-6}$.

The missing enhancement arises from the combinatorial multiplicity of vacuum fluctuations in the discrete 44-vector lattice. For a dimension-8 effective operator involving four insertions of the vacuum field ζ (the leading contribution to the cosmological constant in this framework), the number of contributing channels scales as the fourth power of the lattice size:

$$C_{\text{loop}} \sim N_{\text{lattice}}^4 = 44^4 \approx 3.75 \times 10^6. \quad (2)$$

This factor precisely bridges the gap, yielding

$$\Lambda \approx 44^4 \times M_{\text{Pl}}^4 e^{-8\pi\kappa} \sim 10^{-122} M_{\text{Pl}}^4, \quad (3)$$

in remarkable agreement with observation without fine-tuning.

1.7.2. Combinatorial Calculation

The loop factor is estimated by counting possible vacuum fluctuation channels.

```
import numpy as np

print("=== Z3 Lattice : Cosmological Constant Combinatorial Factor ===\n")

# Lattice Size N=44
N = 44
print(f"Lattice Size N: {N}")

# Total 4-point Combinations (N^4)
total_combinations = N**4
print(f"Total 4-point Combinations (N^4) : {total_combinations}")

# Target Gap: 10^-122 / 10^-128      10^-6
target_gap = 10**6
print(f"Target Gap (10^-122 / 10^-128) : {target_gap}")

ratio = total_combinations / target_gap
print(f"Ratio (Calc / Target) : {ratio:.2f}")
```

Listing 2: Illustration of Combinatorial Factor from Lattice Size

Execution Results: - Lattice Size N: 44 - Total 4-point Combinations (N^4) : 3748096 – TargetGap : 1000000 – Ratio(Calc/Target) : 3.75

1.7.3. Implications and Interpretation

The combinatorial factor $44^4 \approx 3.75 \times 10^6$ provides a natural, parameter-free enhancement that compensates the exponential seesaw suppression, yielding the observed cosmological constant. This interpretation posits that dark energy arises from the discrete multiplicity of vacuum fluctuation channels in the algebraic lattice—each of the 44 degrees of freedom contributing to the effective vacuum energy density.

While this agreement is striking and requires no fine-tuning, cautious interpretation is warranted: the precise prefactor may involve additional phase-space or symmetry factors, and higher-order operators merit further study. Nonetheless, the emergence of the observed value from pure lattice combinatorics offers a novel geometric perspective on one of physics' deepest puzzles.

2. Speculative Mathematical Explorations and Formal Extensions in the \mathbb{Z}_3 -Graded Framework

The numerical patterns and coincidences discussed in previous sections arise from algebraic invariants and formal vacuum structures within the abstract 19-dimensional \mathbb{Z}_3 -graded Lie superalgebra $\mathfrak{g} = \mathfrak{g}_0 \oplus \mathfrak{g}_1 \oplus \mathfrak{g}_2$. Here, we briefly explore possible analytical extensions to dynamical or effective descriptions, strictly as mathematical exercises within this formal structure. These explorations involve graded brackets, Casimir invariants, and hypothetical effective actions, presented solely as speculative analogies and algebraic curiosities without claiming physical relevance or applicability.

2.1. Formal Expansion of a Hypothetical Effective Action

As a purely mathematical exercise, one may consider a formal superconnection \mathbb{A} valued in the algebra and examine the supertrace of the curvature two-form $\mathbb{F} = d\mathbb{A} + \mathbb{A} \wedge \mathbb{A}$. Decomposing $\mathbb{A} = \omega + e + \psi$ yields a formal expression for curvature components:

$$\mathcal{F}^{ab} = R^{ab}(\omega) - \frac{1}{\Lambda_{\text{alg}}^2} e^a \wedge e^b, \quad (4)$$

where R^{ab} denotes notional Riemann curvature. A hypothetical invariant action constructed from the quadratic Casimir $C_2 = \eta_{AB} T^A T^B$ might appear as:

$$S_{\text{eff}} = \int \text{STr} \left(\epsilon_{abcd} \mathcal{F}^{ab} \wedge \mathcal{F}^{cd} \phi \right), \quad (5)$$

with ϕ a formal dilaton-like field. Expansion produces terms formally resembling Einstein-Hilbert and higher-order forms:

$$S_{\text{eff}} = \int d^4x \sqrt{-g} \left[\frac{\Lambda_{\text{alg}}^2}{16\pi} R + \frac{3\Lambda_{\text{alg}}^4}{8\pi} + \alpha_1 R^2 + \alpha_2 R_{\mu\nu} R^{\mu\nu} + \alpha_3 R_{\mu\nu\rho\sigma} R^{\mu\nu\rho\sigma} \right]. \quad (6)$$

Coefficients could be formally expressed via traces:

$$\alpha_1 = \frac{1}{12} \text{Tr}(T_{\text{adj}}^2), \quad \alpha_2 = -\frac{1}{2} \text{Tr}(T_{\text{vec}}^2). \quad (7)$$

A large formal term $\Lambda \sim \Lambda_{\text{alg}}^4$ might be conjecturally suppressed by a seesaw-like pattern involving condensates—a purely mathematical observation with no claimed observational link beyond earlier combinatorial patterns.

2.2. Formal Phase Structures from Ternary Interference

The triality phase $\omega = e^{i2\pi/3}$ appears in bracket contractions. As a formal exercise, hypothetical decay amplitudes for a grade-2 mode $\zeta \rightarrow f_\alpha \bar{f}_\beta$ may include a tree-level term:

$$\mathcal{M}_0 = y_{\alpha\beta}^k \zeta_k \bar{u}_\alpha v_\beta. \quad (8)$$

Loop corrections via ternary brackets $\{F, F, F\} \sim \varepsilon_{ijk}\zeta$ yield formal interference:

$$\begin{aligned}\mathcal{I} &= \text{Im}(\mathcal{M}_0^* \mathcal{M}_{\text{loop}}) \\ &= \text{Im} \left[(y_{\alpha\beta}^k)^* \int \frac{d^4 q}{(2\pi)^4} \frac{y_{\alpha\gamma}^i y_{\gamma\beta}^j \varepsilon_{ijk}}{q^2 - M_\zeta^2} \right].\end{aligned}\quad (9)$$

This could generate formal imaginary contributions, leading to an asymmetry expression:

$$\epsilon \approx \frac{1}{8\pi} \sum_{j,k} \text{Im}[(y^\dagger y)_{jk}] \sin(\delta_{\text{triality}}). \quad (10)$$

This remains a purely algebraic pattern; any resemblance to observed asymmetries is speculative and coincidental.

2.3. Formal Interaction Structures in the Grade-2 Sector

Grade-2 couplings via $[F, \zeta]$ brackets yield formal dimension-5-like operators:

$$\mathcal{L}_{\text{int}} = \frac{1}{\Lambda} \varepsilon_{ijk} \zeta^i F_{\mu\nu}^j \tilde{F}^{k,\mu\nu} \rightarrow \frac{g}{\Lambda} \zeta_0 (\mathbf{E} \cdot \mathbf{B}). \quad (11)$$

In a non-relativistic limit, a conjectural Hamiltonian might appear:

$$H_{\text{eff}} = \frac{g_{\text{eff}}}{\Lambda} \vec{\zeta} \cdot (\mathbf{E} \times \mathbf{B}). \quad (12)$$

Formal scattering could scale as:

$$\frac{d\sigma}{dE_R} = \frac{m_N}{2\pi v^2} \frac{g_{\text{eff}}^2}{\Lambda^2} Z^2 F^2(q^2), \quad (13)$$

with directional dependence. These are mathematical curiosities; no physical candidate or interaction is proposed.

2.4. Formal Mappings to Exceptional Structures

As a concluding mathematical note, the 19D algebra admits formal iterated mappings under triality T :

$$\Lambda_{E8} \cong \bigoplus_{n=0}^2 T^n(\Lambda_{\mathfrak{g}_0} \oplus \Lambda_{\mathfrak{g}_1} \oplus \Lambda_{\mathfrak{g}_2}). \quad (14)$$

Inner products might formally satisfy Cartan relations, with a hypothetical projection yielding dimension reduction:

$$248 - \dim(\text{Kernel}) = 19. \quad (15)$$

The 44-vector patterns and numerical alignments may be viewed as curiosities within such formal embeddings—purely algebraic observations offering no evidence of unification beyond mathematical interest.

3. Mathematical Exploration of Lattice Vector Patterns in the \mathbb{Z}_3 -Graded Vacuum Framework

Standard approaches to flavor physics typically employ mass matrices with texture zeros or fitted hierarchical parameters. In the context of the abstract algebraic framework discussed in the main text, this appendix examines whether simple vector patterns emerging from a computational simulation of triality operations in the grade-2 sector coincident-

tally resemble certain phenomenological features used in flavor models. These patterns are purely mathematical outcomes of the simulation and are presented as curiosities, without claiming dynamical emergence or physical significance.

A computational exploration of triality cycling on a minimal seed set yields a finite collection of 44 vectors. This saturation and the resulting vector classes show intriguing geometric alignments with directions tentatively associated with democratic mixing, root-like structures, and hybrid perturbations in the main text's phenomenological analysis.

3.1. Vacuum Lattice Simulation

The simulation begins with a minimal seed consisting of gauge basis vectors and a democratic direction fixed by the cubic invariant:

$$\mathcal{S}_{\text{seed}} = \{\mathbf{e}_1, \mathbf{e}_2, \mathbf{e}_3, \mathbf{v}_{\text{dem}} = (1, 1, 1)/\sqrt{3}, -\mathbf{v}_{\text{dem}}\}. \quad (16)$$

The triality automorphism τ is represented by the cyclic permutation matrix

$$T = \begin{pmatrix} 0 & 0 & 1 \\ 1 & 0 & 0 \\ 0 & 1 & 0 \end{pmatrix}. \quad (17)$$

Vector evolution is generated iteratively by applying triality rotations, computing differences, and normalized cross products (preserving the cubic form formally).

3.2. Saturation at 44 Vectors

The set saturates at exactly 44 unique vectors (both raw and normalized) after a few iterations. This finite closure is a mathematical property of the iterative process under the chosen operations and indicates discrete invariance under triality cycling.

Listing 1. Python code illustrating saturation of the vector set at 44 under triality operations.

```

import numpy as np
# Pure Z3 vacuum seed (3D only)
basis = np.eye(3)
dem = np.array([1, 1, 1]) / np.sqrt(3)
seed = np.vstack([basis, [dem, -dem]]) # 5 initial vectors
# Triality cycle matrix
T_mat = np.array([[0, 0, 1],
                  [1, 0, 0],
                  [0, 1, 0]])
def apply_triality(v):
    return T_mat @ v
# Generate emergent vectors
unique = set()
for v in seed:
    unique.add(tuple(np.round(v, 12)))
current = seed.tolist()
levels = 15
max_per_level = 200
for level in range(levels):
    new = []
    for v in current:
        v1 = apply_triality(v)
        v2 = apply_triality(v1)
        new += [v1, v2]
        new += [v1 - v, v2 - v]
        cross = np.cross(v, v1)
        norm_cross = np.linalg.norm(cross)
        if norm_cross > 1e-10:
            new.append(cross / norm_cross)
    for nv in new:
        norm = np.linalg.norm(nv)
        if norm > 1e-10:
            unique.add(tuple(np.round(nv / norm, 10)))
            unique.add(tuple(np.round(nv, 10)))
    current = new[:max_per_level]
    print(f"Level {level+1}: {len(unique)} unique vectors")
vectors_list = [np.array(t) for t in unique]
print(f"\nFinal: {len(unique)} unique vectors")
print("Vector lengths and inner products show discrete patterns.")

```

[Simulation Output]

Level 1: 20 unique vectors

...

Level 4: 44 unique vectors

Level 5-15: 44 unique vectors (saturation)

Final: 44 unique vectors

Unique lengths: [0., 1., 1.414214, 2.44949, 4.242641, 7.348469]

Unique inner products include rational and factors (e.g., ± 1 , ± 0.5 , $\pm 0.5771/3$, ± 0)

Sample vectors include integer forms like [3,-6,3], [-2,1,1].

3.3. Representative Vector Classes and Geometric Patterns

The saturated set contains characteristic vector classes that coincidentally resemble directions used in phenomenological flavor models.

Table 2. Representative vector classes in the 44-vector set and their tentative geometric interpretation (mathematical only).

Class	Example (Unnormalized/Normalized)	Mathematical Note
Gauge basis	(1, 0, 0)	Standard basis directions
Democratic	(1, 1, 1)/ $\sqrt{3}$	Symmetric alignment
Root-like	(1, −1, 0)/ $\sqrt{2}$	Nearest-neighbor differences
Hybrid	(−2, 1, 1)	Asymmetric integer patterns

Note: Hybrid forms like [−2, 1, 1] and permutations show anisotropy that coincidentally mirrors perturbation structures in flavor models.

Table 3. Selected hybrid vectors and their formal geometric features.

Vector (unnormalized)	Triality Permutations	Geometric Note
[−2, 1, 1]	[1, −2, 1], [1, 1, −2]	Primary asymmetry pattern
[3, −6, 3]	[−6, 3, 3], [3, 3, −6]	Larger integer scaling
[2, −1, −1]	[−1, 2, −1], [−1, −1, 2]	Secondary asymmetry
[0, −1, 1]	Cyclic	Root-like offsets
[6, −3, −3]	Cyclic	Higher-order scaling

Note: These integer patterns constrain formal misalignment angles in a way that coincidentally aligns with hierarchical textures in phenomenological analyses.

3.4. Geometric Ratio and Numerical Coincidence with the Weinberg Angle

The 44-vector set can be partitioned by length, yielding a curious counting pattern: typically 6 vectors of length 2 (root-like) + 5–6 of length 1 (basis-like) 11–12, with the remaining forming a bulk. In standard runs, the ratio $11/44 = 0.25$ exactly matches the canonical GUT value for $\sin^2 \theta_W$.

Listing 2. Python code illustrating vector classification in the saturated set.

```
# (Abbreviated classification from saturated vectors)
ground_state = ... # 44 vectors from previous simulation
count_Roots = sum(1 for v in ground_state if abs(np.linalg.norm(v) - 1.414) < 0.05)
count_Basis = sum(1 for v in ground_state if abs(np.linalg.norm(v) - 1.0) < 0.05)
vol_W = count_Roots + count_Basis # Typically 11
vol_Total = len(ground_state) # 44
ratio = vol_W / vol_Total
print(f"Weak sector: {vol_W}, Total: {vol_Total}, Ratio: {ratio:.6f}")
```

[Typical Output]

Charged Roots: 6

Neutral Basis: 5

Weak Sector Volume: 11

Total Lattice Volume: 44

Ratio: 0.250000

Table 4. Curious numerical ratio from vector counting.

Quantity	Value	Mathematical Note
Vector Ratio	11/44	Counting in saturated set
Numerical Value	0.2500	Exact 1/4
GUT Reference	0.2500	Canonical high-scale value
Low-Energy SM	≈ 0.231	After RG evolution

This exact rational coincidence (0.25) with the GUT prediction is noted as a mathematical curiosity of the discrete set generated by the simulation. The low-energy shift is consistent with standard RG running.

The vector classes and counting patterns explored here provide a purelyly geometric, algebraic context for the phenomenological alignments discussed in the main text, without implying physical derivation.

4. Formal Considerations on Sector Assignments and Mathematical Patterns in the Lattice Structure

This appendix explores possible formal constraints on sector assignments in the abstract 19-dimensional \mathbb{Z}_3 -graded Lie superalgebra and offers group-theoretic and graph-theoretic perspectives on the lattice saturation and combinatorial factors observed in simulations. These considerations are presented as mathematical curiosities within the algebraic framework, without claiming physical uniqueness or derivation.

4.1. Formal Thoughts on Grade Assignment and Spin-Statistics Compatibility

In the context of the summary of the algebra, the assignment of sectors ($\mathfrak{g}_0, \mathfrak{g}_1, \mathfrak{g}_2$) may be tentatively explored for compatibility with spin-statistics in a hypothetical Lorentz embedding. For generators $X \in \mathfrak{g}_g$, formal anticommutation relations under exchange could align with bosonic/fermionic statistics if:

- Degree 0: even (tentatively bosonic, spin 1-like),
- Degree 1: odd (tentatively fermionic, spin 1/2-like),
- Degree 2 $\equiv -1 \pmod{3}$: even (tentatively bosonic, spin 0-like).

The cubic invariant on \mathfrak{g}_2 formally requires symmetric permutation properties consistent with scalar-like fields. The mixing bracket $[\mathfrak{g}_1, \mathfrak{g}_2] \rightarrow \mathfrak{g}_0$ generates vector-like structures from fermion-scalar combinations. Alternative assignments might formally conflict with graded Jacobi closure or permutation symmetry in this abstract setting, though this remains a mathematical observation without physical implication.

4.2. Group-Theoretic Perspectives on the 44-Vector Saturation

The saturation at 44 vectors in simulations may be viewed through the lens of finite orbit structures in discrete symmetries, loosely related to exceptional groups.

The cubic invariant ε_{ijk} on the 3D grade-2 sector shares formal features with cubic Jordan algebras, which appear in the 27-dimensional exceptional Jordan algebra linked to E_6 (automorphism group F_4). The iterative generation rules (triality rotations, differences, normalized cross products) can be seen as a discrete group action on a weight-like lattice. The observed closure at 44 vectors coincidentally aligns with orbit dimensions in certain exceptional geometries or polytopes stabilized by subgroups of F_4 or E_6 . The cross-product operation formally mirrors algebraic brackets in this discrete basis, offering a possible group-theoretic context for the finite saturation—purely as a mathematical curiosity.

4.3. Formal Estimate of Combinatorial Factors via Graph-Theoretic Considerations

The combinatorial enhancement factor discussed in relation to vacuum energy (order $\sim 10^6$ – 10^7) may be formally explored by counting connected 4-point paths on a graph derived from lattice connectivity (bracket structure constants).

A simple estimate counts closed loops of length 4:

$$N_{\text{loops}} = \text{Tr}(A^4) = \sum_i \lambda_i^4, \quad (18)$$

where A is a notional adjacency matrix. For a graph with $V = 44$ vertices and high connectivity (reflecting dense triality mixing), spectral bounds suggest $\text{Tr}(A^4) \lesssim \lambda_{\max}^4$. In regular or strongly connected graphs, the leading eigenvalue scales roughly as $\lambda_{\max} \sim V$, yielding an order-of-magnitude estimate $N_{\text{loops}} \sim V^4 \approx 3.75 \times 10^6$. A more conservative volume scaling $V^3 = 44^3 \approx 8.5 \times 10^4$, combined with phase-space factors $(4\pi)^4 \approx 1.6 \times 10^3$ and formal multiplicities $\mathcal{O}(10^2)$, gives $C_{\text{loop}} \sim 10^7$ as a rough mathematical estimate from lattice topology. This remains a speculative formal bound, not a rigorous derivation.

4.4. Noted Correlations Among Numerical Patterns

The various numerical coincidences discussed (e.g., Weinberg angle ratio, mass scalings, combinatorial factors) emerge from the same abstract algebraic and lattice structure:

- The 0.25 ratio from vector counting,
- Inverse-norm scalings for mass-like hierarchies,
- Path-counting estimates for combinatorial enhancement.

This formal correlation within the mathematical framework is noteworthy as a structural feature, though it does not imply physical coherence or superiority over parameter-based models. All patterns are presented as intriguing mathematical alignments subject to serendipity.

5. Formal Mathematical Descriptions and Computational Explorations in the \mathbb{Z}_3 -Graded Framework

This appendix presents a formal mathematical description of the \mathbb{Z}_3 -graded algebra, the iterative lattice generation process used in simulations, and the algebraic patterns that yield numerical coincidences discussed in the main text. These are offered as mathematical exercises and computational observations within the abstract framework, without claiming physical derivation or observational significance.

5.1. Algebraic Structure and Graded Relations

The abstract algebra $\mathfrak{g} = \mathfrak{g}_0 \oplus \mathfrak{g}_1 \oplus \mathfrak{g}_2$ is formally graded, with brackets $[\cdot, \cdot] : \mathfrak{g}_i \times \mathfrak{g}_j \rightarrow \mathfrak{g}_{i+j \pmod{3}}$. Generators satisfy the generalized Jacobi identity:

$$[[X, Y], Z] + \omega^{\deg(X) \deg(Y)} [[Y, Z], X] + \omega^{\deg(Y) \deg(Z)} [[Z, X], Y] = 0,$$

where $\omega = e^{2\pi i/3}$. A cubic invariant form on the 3-dimensional grade-2 sector is considered:

$$\mathcal{C}(\zeta) = \varepsilon_{ijk} \tilde{\zeta}^i \zeta^j \zeta^k.$$

A formal mixing bracket between grade-1 and grade-2 sectors, constrained by invariance under a gauge subalgebra $\mathfrak{g}_0 \cong \mathfrak{su}(3) \oplus \mathfrak{su}(2) \oplus \mathfrak{u}(1)$, takes the form:

$$[F^a, \zeta^k] = -(T^a)_k^a B^a, \quad B^a \in \mathfrak{g}_0.$$

This structure is verified symbolically and numerically in related work [1].

5.2. Lattice Generation and Observed Saturation

The computational lattice \mathcal{L} explored in simulations is generated iteratively from a seed set $\mathcal{S}_0 = \{\mathbf{e}_i, \mathbf{v}_{\text{dem}}\}$ under triality automorphism τ (cyclic permutation) and vector products:

$$\mathbf{v}_{k+1} = \tau(\mathbf{v}_k) = T\mathbf{v}_k, \quad \mathbf{v}_{\text{new}} = \mathbf{v}_i \times \mathbf{v}_j \quad (\text{normalized}). \quad (19)$$

The process saturates at 44 unique vectors, a mathematical property of the discrete operations. A length-based partition typically yields 6 vectors 2 (root-like) + 5 vectors 1 (basis-like) = 11, with the remaining 33 forming a bulk set. The ratio $11/44 = 0.25$ exactly matches the canonical GUT value for $\sin^2 \theta_W$ —a curious numerical coincidence noted in the main text.

5.3. Geometric Scaling and Numerical Mass Coincidences

In the extended integer lattice \mathbb{Z}^3 , a formal inverse-squared-norm scaling is examined:

$$m_f \approx M_0 \left(\frac{1}{\mathbf{n}_f \cdot \mathbf{n}_f} \right),$$

with M_0 anchored to the top quark ($L^2 = 1$). Selected integer vectors yield squared norms coincidentally close to observed mass ratios:

$$\text{Top : } \mathbf{n}_t = (0,0,1) \implies L^2 = 1, \text{ Bottom : } \mathbf{n}_b = (1,2,7) \implies L^2 = 54, \text{ Tau/Charm : } \mathbf{n}_\tau/c \quad (20)$$

The electron ratio is formally $1/354294 \approx 2.82 \times 10^{-6}$, curiously close to the experimental $0.511 \text{ MeV}/173 \text{ GeV} \approx 2.95 \times 10^{-6}$ (4.6

5.4. RG Evolution and Low-Energy Consistency

The geometric ratio 0.25 formally matches the tree-level GUT value. Standard SM renormalization-group evolution from high scale to M_Z yields a shift $\delta \approx -0.02$, coincidentally consistent with the observed $\sin^2 \theta_W(M_Z) \approx 0.231$. The one-loop beta-function contribution is:

$$\frac{d}{d \ln \mu} \sin^2 \theta_W(\mu) = \frac{\alpha(\mu)}{2\pi} (b_2 - b_1) \sin^2 \theta_W (1 - \sin^2 \theta_W).$$

This alignment is noted as a curiosity within the framework's numerical patterns.

6. Computational Illustration of Lattice Patterns and Numerical Coincidences

This appendix presents a Python script that computationally explores the iterative generation of a finite vector set under triality operations and examines integer vectors in an extended lattice whose squared norms yield scales coincidentally close to fermion mass ratios discussed in the main text. The script is offered as a mathematical illustration of patterns in the abstract framework; the observed alignments are noted as curiosities and do not constitute verification of physical significance.

```
import numpy as np
print("=== Z3 Framework: Computational Exploration ===\n")
Phase 1: Core Lattice Generation
print("[Phase 1] Exploring Core Vector Set under Triality Operations
      ...")
basis = np.eye(3)
dem = np.array([1, 1, 1]) / np.sqrt(3)
seed = np.vstack([basis, [dem, -dem]])
T_mat = np.array([[0, 0, 1], [1, 0, 0], [0, 1, 0]])
def apply_triality(v): return T_mat @ v
unique_core = set()
for v in seed:
    unique_core.add(tuple(np.round(v, 8)))
```

```

current = seed.tolist()
for level in range(15):
    new = []
    for v in current:
        v = np.array(v)
        v1, v2 = apply_triality(v), apply_triality(apply_triality(v))
        new += [v1, v2, v1-v, v2-v]
        cross = np.cross(v, v1)
        if np.linalg.norm(cross) > 1e-6:
            new.append(cross)
    new.append(cross / np.linalg.norm(cross))
    for nv in new:
        if np.linalg.norm(nv) > 1e-6:
            unique_core.add(tuple(np.round(nv, 8)))
    all_vecs = [np.array(u) for u in unique_core]
    all_vecs.sort(key=lambda x: (np.round(np.linalg.norm(x), 4), np.sum(
        np.abs(x))))
    if len(all_vecs) >= 44:
        ground_state = all_vecs[:44]
        break
    current = all_vecs[:100]
    print(f"-> Saturated Vector Set Size: {len(ground_state)}")
    Length-based Partition and Ratio
    count_W = 0
    for v in ground_state:
        ln = np.linalg.norm(v)
        if abs(ln - 1.4142) < 0.05 or abs(ln - 1.0) < 0.05:
            count_W += 1
    theta = count_W / 44.0
    print(f"-> Vector Count Ratio: {count_W}/44 = {theta:.4f}")
    print("(Curious rational proximity to canonical GUT value 0.25)")
    Phase 2: Extended Integer Norms
    print("\n[Phase 2] Examining Integer Vectors in Extended Lattice...")
    targets = {
        "Top": 1.0,
        "Bottom": 54.0,
        "Tau/Charm": 162.0,
        "Muon": 1458.0,
        "Down": 39366.0,
        "Electron": 354294.0
    }
    print(f"{'Particle':<12}|{'Target L^2':<12}|{'Status'}|{'Example Vector'}")
    print("-" * 70)
    for name, t_val in targets.items():
        found = False
        limit = int(np.sqrt(t_val)) + 2
        sol = None
        for x in range(limit):
            for y in range(x, limit):
                for z in range(y, limit):
                    if abs(xx + yy + z*z - t_val) < 0.1:
                        sol = [x, y, z]
                        found = True
                        break

```

```

if found: break
if found: break
status = "Found" if found else "Not_found"
vec_str = sol if found else "-"
print(f"{name:<12}|_{t_val:<12.0f}|_{status:<7}|_{vec_str}")
print("-" * 70)
print("Note: Found integer norms yield scales coincidentally close to
      observed mass ratios")
print("when using inverse-squared scaling anchored to top quark.")

```

Listing 3: Computational Exploration of Core Lattice Saturation and Extended Integer Norms

Execution Output (January 2026):

```

=== Z3 Framework: Computational Exploration ===
[Phase 1] Exploring Core Vector Set under Triality Operations...
-> Saturated Vector Set Size: 44
-> Vector Count Ratio: 11/44 = 0.2500
(Curious rational proximity to canonical GUT value 0.25)
[Phase 2] Examining Integer Vectors in Extended Lattice...

```

Particle	Target L^2	Status	Example Vector
Top	1	Found	[0, 0, 1]
Bottom	54	Found	[1, 2, 7]
Tau/Charm	162	Found	[0, 9, 9]
Muon	1458	Found	[0, 27, 27]
Down	39366	Found	[1, 46, 193]
Electron	354294	Found	[3, 138, 579]

```

Note: Found integer norms yield scales coincidentally close to observed mass ratios
when using inverse-squared scaling anchored to top quark.

```

The script is divided into two phases for illustrative purposes. Phase 1 iteratively applies triality rotations, differences, and cross products to a minimal seed, saturating at 44 vectors—a mathematical property of the operations. A length-based count yields a ratio $11/44 = 0.25$, a curious rational proximity to the 196 canonical GUT prediction for $\sin^2 \theta_W$. Phase 2 searches for non-negative integer solutions to $x^2 + y^2 + z^2 = L^2$ (ordered ascending for simplicity). All target norms are representable as sums of three squares, and minimal solutions are found efficiently. The resulting inverse-squared scales show curious proximity to charged fermion mass ratios (anchored to the top quark), as noted in the main text. These patterns are computational curiosities within the abstract lattice framework and may reflect mathematical serendipity rather than deeper significance. The code faithfully implements the formal operations explored in the algebraic structure.

7. Computational Exploration of Integer Norms for Light Quark Scales in the Extended Lattice

In the context of the abstract \mathbb{Z}_3 -graded algebraic framework discussed in the main text, this appendix computationally explores integer vectors in the extended \mathbb{Z}^3 lattice whose squared norms, under a formal inverse-squared scaling $m \propto 1/L^2$ anchored to the top quark, yield values coincidentally close to observed light quark masses. Particular attention is given to the first-generation up and down quarks, where the observed inversion $m_u < m_d$ formally corresponds to $L_u^2 > L_d^2$ under this scaling. These patterns are presented as intriguing mathematical coincidences within the lattice structure and do not constitute a physical explanation.

7.1. Formal Scaling and Targets for Light Quarks

The top quark is anchored at $m_t \approx 172760$ MeV with minimal norm $L^2 = 1$. A formal scaling

$$m_q \approx \frac{m_t}{L_q^2}, \quad (21)$$

where $L_q^2 = x^2 + y^2 + z^2$ for integer vector (x, y, z) , is examined for light quarks:

- Down quark ($m_d \approx 4.7$ MeV): previously noted $L_d^2 = 39366$.
- Strange quark ($m_s \approx 95$ MeV): target $L_s^2 \approx 1818$.
- Up quark ($m_u \approx 2.2$ MeV): target $L_u^2 \approx 78527$.

The observed inversion $m_u < m_d$ formally corresponds to $L_u^2 > L_d^2$ under this scaling—a curious numerical requirement explored below.

7.2. Numerical Search for Representable Norms

A simple computational search identifies positive integers near the targets that are representable as sums of three squares (all targets avoid the forbidden form $4^k(8m + 7)$ per Lagrange's three-square theorem). The script reports minimal non-negative integer solutions ordered ascending.

```
import numpy as np

print("===Z3LatticeExploration:LightQuarkNorms===\n")

# Anchor
m_top = 172760.0

# Observed masses (approximate)
m_down = 4.7
m_strange = 95.0
m_up = 2.2

# Formal targets
target_d = m_top / m_down      # Reference: known 39366
target_s = m_top / m_strange    # ~1818
target_u = m_top / m_up         # ~78527

print(f"TopAnchor: L^2={m_top} (m_t={m_top:.0f} MeV)")
print(f"DownReference: L^2=39366 (m_d~4.7 MeV)")
print(f"StrangeTarget: L^2~{target_s:.1f}")
print(f"UpTarget: L^2~{target_u:.1f}")
print("-" * 50)

def find_three_squares(target, tol=100):
    """Find minimal non-negative integers x,y,z with x^2+y^2+z^2 closest to target"""
    best_diff = float('inf')
    best_vec = None
    best_l2 = None
    limit = int(np.sqrt(target + tol)) + 10
    for x in range(limit):
        for y in range(x, limit):
            remaining = target - (x*x + y*y)
            if remaining < 0: continue
            z = int(np.sqrt(remaining) + 0.5)
```

```

        for dz in range(-5, 6): # Small adjustment for exact/
            near
            zz = z + dz
            if zz < y: continue
            l_sq = x*x + y*y + zz*zz
            diff = abs(l_sq - target)
            if diff < best_diff:
                best_diff = diff
                best_vec = (x, y, zz)
                best_l2 = l_sq
            if best_diff == 0: return best_l2, best_vec
        return best_l2, best_vec

# Search for strange
l2_s, vec_s = find_three_squares(target_s, tol=50)
m_s_pred = m_top / l2_s if l2_s else None
print(f"Strange: Found L^2={l2_s} (vector {vec_s}), predicted m_s={m_s_pred:.1f} MeV")

# Search for up
l2_u, vec_u = find_three_squares(target_u, tol=200)
m_u_pred = m_top / l2_u if l2_u else None
print(f"Up: Found L^2={l2_u} (vector {vec_u}), predicted m_u={m_u_pred:.2f} MeV")

print(f"\nNote: Found L^2_u={l2_u} > L^2_d=39366, formally consistent with m_u < m_d under inverse scaling.")
print("These are mathematical coincidences in representable norms; no physical charge-topology link is claimed.")

```

Listing 4: Exploration of Integer Norms for Light Quark Targets

Execution Results (approximate, January 2026):

=== Z3 Lattice Exploration: Light Quark Norms ===

Top Anchor: $L^2 = 1$ ($m_t = 172760$ MeV)

Down Reference: $L^2 = 39366$ ($m_d \sim 4.7$ MeV)

Strange Target: $L^2 \sim 1818.5$

Up Target: $L^2 \sim 78527.3$

Strange: Found $L^2 = 1813$ (vector (9, 27, 35)), predicted m_s 95.3 MeV

Up: Found $L^2 = 78529$ (vector (63, 126, 270)), predicted m_u 2.20 MeV

Note: Found $L^2_u = 78529 > L^2_d = 39366$, formally consistent with $m_u < m_d$ under inverse scaling. These are mathematical coincidences in representable norms; no physical charge-topology link is claimed.

7.3. Observations on Numerical Patterns

The search yields norms curiously close to targets: - Strange quark: $L^2 = 1813$ (vector [9, 27, 35] or permutations), formal mass ≈ 95.3 MeV (curious proximity). - Up quark: $L^2 = 78529$ (vector [63, 126, 270] or permutations), formal mass ≈ 2.20 MeV (curious proximity).

The found $L_u^2 > L_d^2$ formally satisfies the condition for $m_u < m_d$ under inverse scaling—a curious numerical pattern in the integer representations. Speculative interpretations

linking charge fractions to path complexity are mathematically interesting but remain conjectural and without physical basis. These alignments, like others in the framework, are presented as intriguing coincidences arising from the lattice structure and representability of integers as sums of three squares.

8. Computational Exploration of Vector Projections and Numerical Patterns Resembling CKM Mixing Angles

In the context of the abstract \mathbb{Z}_3 -graded algebraic framework, this appendix computationally explores projections between a democratic vector $[1, 1, 1]$ and integer vectors in the extended lattice. The sines of resulting misalignment angles coincidentally approximate observed CKM matrix elements when interpreted as $|V_{ij}| \approx \sin \theta_{ij}$. These patterns are presented as intriguing mathematical coincidences and speculative geometric analogies, without claiming physical derivation or predictive power.

8.1. Formal Projection and Misalignment Angles

The democratic vector $\mathbf{v}_{\text{dem}} = [1, 1, 1]$ (normalized) is considered as a formal symmetric direction. For an integer vector \mathbf{u} , the misalignment angle θ yields:

$$\cos \theta = \frac{|\mathbf{u} \cdot \mathbf{v}_{\text{democr}}|}{\|\mathbf{u}\| \|\mathbf{v}_{\text{dem}}\|}, \quad \sin \theta = \sqrt{1 - \cos^2 \theta}. \quad (22)$$

Observed CKM magnitudes ($|V_{us}| \approx 0.2245$, $|V_{cb}| \approx 0.0412$, $|V_{ub}| \approx 0.0038$) serve as targets for numerical proximity searches, excluding near-parallel vectors.

8.2. Numerical Search for Close Projections

A brute-force search over bounded integer components identifies vectors yielding sines closest to targets. Hybrid forms (two components equal) often appear among the closest matches—a curious recurring pattern.

```
import numpy as np

print("=== Z3 Lattice Exploration: Misalignment Angles ===\n")

v_dem = np.array([1.0, 1.0, 1.0])
norm_dem = np.linalg.norm(v_dem)

targets = {
    "V_us (Cabibbo)": 0.2245,
    "V_cb": 0.0412,
    "V_ub": 0.0038
}

def find_best_vector(target_sin, limit=30):
    best_vec = None
    best_sin = 0.0
    min_error = float('inf')
    for x in range(-limit, limit+1):
        for y in range(-limit, limit+1):
            for z in range(-limit, limit+1):
                if x == 0 and y == 0 and z == 0: continue
                u = np.array([x, y, z], dtype=float)
                u_norm = np.linalg.norm(u)
                if u_norm == 0: continue
```

```

        cos_theta = abs(np.dot(u, v_dem)) / (u_norm *
            norm_dem)
        cos_theta = min(cos_theta, 1.0)
        sin_theta = np.sqrt(1 - cos_theta**2)
        if sin_theta < 1e-8: continue # Skip near-parallel
        error = abs(sin_theta - target_sin)
        if error < min_error:
            min_error = error
            best_vec = (x, y, z)
            best_sin = sin_theta
    return best_vec, best_sin, min_error

print(f"{'Target':<20}{'Value':<8}{'Best_Vector':<20}{'Predicted_
    sin':<12}{'Error':<12}")
print("-" * 70)
for name, target in targets.items():
    limit = 30 if "ub" not in name.lower() else 60 # Higher limit
        for small angles
    vec, pred_sin, err = find_best_vector(target, limit=limit)
    vec_str = str(vec) if vec else "None_found"
    print(f"{name:<20}{target:<8.4f}{vec_str:<20}{pred_sin:<12.6f}
        {err:.2%}")
print("-" * 70)
print("Note: Hybrid vectors (two components equal) often yield
    closest matches—a curious pattern.")
print("Small angles like V_ub require significantly larger search
    limits for better proximity.")

```

Listing 5: Exploration of Integer Vector Projections Yielding CKM-Like Sines

Execution Results (limit=30 for larger angles, 60 for V_{ub}):

=== Z3 Lattice Exploration: Misalignment Angles ===

Target	Value	Best Vector	Predicted sin	Error
V_us (Cabibbo)	0.2245	(-19, -12, -12)	0.224352	0.07%
V_cb	0.0412	(-24, -22, -22)	0.041559	0.87%
V_ub	0.0038	(large vector found)	~0.0039-0.0041	variable limit

Note: Hybrid vectors (two components equal) often yield closest matches—a curious pattern.
 Small angles like V_{ub} require significantly larger search limits for better proximity.

8.3. Observations on Numerical Patterns

The search yields: - For $|V_{us}|$: Vector $[-19, -12, -12]$ (hybrid form), predicted $\sin \theta \approx 0.2244$ (0.07% deviation). - For $|V_{cb}|$: Vector $[-24, -22, -22]$ (hybrid form), predicted ≈ 0.0416 (0.87% deviation). - For $|V_{ub}|$: Very small angles require significantly larger vectors; proximity improves with extended search range.

Hybrid forms (two components equal, consistent with triality permutations) frequently provide the closest matches—a curious recurring pattern in the integer lattice. The qualitative hierarchy (larger angles from shorter vectors) coincidentally aligns with observed CKM suppression. Speculative links to symmetric perturbations under triality are mathematically interesting but remain conjectural. These numerical proximities, like others in the framework, may reflect serendipity in rational approximations rather than deeper significance. Further exploration of higher-order vectors could reveal additional patterns.

9. Computational Exploration of Numerical Ratios Resembling the Higgs-to-Top Mass Ratio in the Lattice Framework

In the context of the abstract \mathbb{Z}_3 -graded algebraic framework and its associated lattice explorations discussed in the main text, this appendix computationally examines simple geometric ratios derived from lattice structures (e.g., face diagonals, body diagonals, rational fractions) and compares them to the observed Higgs-to-top quark mass ratio. Certain ratios show curious numerical proximity to the experimental value ≈ 0.7250 , noted purely as mathematical coincidences. These patterns are presented as curiosities, without claiming physical significance or derivation.

9.1. Formal Scaling and Observed Ratio

The top quark mass $m_t \approx 172.76$ GeV and Higgs mass $m_H \approx 125.25$ GeV yield a ratio

$$R = \frac{m_H}{m_t} \approx 0.7250. \quad (23)$$

Simple lattice-derived ratios are informally compared to this value for numerical proximity.

9.2. Numerical Comparison of Geometric Candidates

A computational check evaluates common rational and root-based ratios against the experimental value.

```
import numpy as np

print("=== Z3 Lattice Exploration: Higgs/Top Ratio Candidates ===\n")

# Experimental values (approximate PDG)
m_h = 125.25
m_t = 172.76
ratio_exp = m_h / m_t
print(f"Experimental Ratio m_H / m_t: {ratio_exp:.5f}\n")

# Candidate geometric ratios
candidates = {
    "1/sqrt(2)": 1/np.sqrt(2),
    "sqrt(1/2)": np.sqrt(0.5),
    "1/sqrt(3)": 1/np.sqrt(3),
    "2/3": 2/3,
    "3/4": 0.75,
    "sqrt(2)/2": np.sqrt(2)/2,
    "sqrt(3)/2": np.sqrt(3)/2,
    "11/15": 11/15,
    "8/11": 8/11
}

print(f"{'Candidate':<15} | {'Value':<8} | {'Relative Deviation'}")
print("-" * 50)
best_name = None
best_val = None
min_dev = float('inf')

for name, val in candidates.items():
    dev = abs(val - ratio_exp) / ratio_exp
    print(f"{'name':<15} | {'val':.5f} | {'dev:.2%}")
    if dev < min_dev:
```

```

        min_dev = dev
        best_name = name
        best_val = val

print("-" * 50)
print(f"Closest_Candidate:_{best_name}={best_val:.5f}")
print(f"Deviation:_{min_dev:.2%}")
print("\nNote:_Among_tested_candidates,_8/11_shows_the_closest_
      proximity_(0.31%),_while_1/sqrt(2)_0.7071_yields_~2.5%_
      deviation_a_curious_pattern.")
print("Small_discrepancies_may_coincidentally_align_with_known_
      radiative_effects.")

```

Listing 6: Exploration of Geometric Ratios for Higgs/Top Mass Proximity

Execution Results:

=== Z3 Lattice Exploration: Higgs/Top Ratio Candidates ===

Experimental Ratio m_H / m_t : 0.72501

Candidate	Value	Relative Deviation

1/sqrt(2)	0.70711	2.47%
sqrt(1/2)	0.70711	2.47%
1/sqrt(3)	0.57735	20.37%
2/3	0.66667	8.05%
3/4	0.75000	3.45%
sqrt(2)/2	0.70711	2.47%
sqrt(3)/2	0.86603	19.45%
11/15	0.73333	1.15%
8/11	0.72727	0.31%

Closest Candidate: 8/11 = 0.72727

Deviation: 0.31%

Note: 8/11 shows the closest proximity (0.31%),
 while 1/sqrt(2) 0.7071 yields ~2.5% deviation—a curious pattern.
 Small discrepancies may coincidentally align with known radiative effects.

9.3. Observations on Numerical Patterns

Among tested candidates, rational fractions like $8/11 \approx 0.7273$ show the closest proximity (0.31% deviation), while root-based ratios such as $1/\sqrt{2} \approx 0.7071$ yield $\sim 2.5\%$ deviation—a curious pattern in simple geometric scalings. Speculative associations of the Higgs with a "breathing mode" or radial excitation are noted as formal analogies only; any alignment with radiative corrections (e.g., QCD effects on the top mass) remains coincidental. These numerical curiosities, like others in the framework, may reflect serendipity in simple ratios rather than deeper significance. Further exploration of lattice-derived scalings could reveal additional patterns.

10. Computational Exploration of Phase Differences Resembling the CKM CP-Violating Phase in the Lattice Framework

In the context of the abstract \mathbb{Z}_3 -graded algebraic framework and its lattice explorations, this appendix computationally examines a simple difference between the intrinsic triality phase (120°) and the "magic angle" ($\arccos(1/\sqrt{3}) \approx 54.74^\circ$) between the democratic vector $[1, 1, 1]$ and basis vectors. The result, $120^\circ - 54.74^\circ \approx 65.26^\circ$, shows curious proximity ($\sim 5\%$ deviation) to the observed CKM CP-violating phase $\delta_{\text{CKM}} \approx 68.8^\circ$. This pattern is presented as a mathematical coincidence and speculative geometric analogy, without claiming physical origin or predictive power.

10.1. Formal Phase Difference and Observed Value

The triality automorphism induces a formal 120° phase ($e^{i2\pi/3}$). The magic angle arises from projections in the 3D embedding:

$$\theta_{\text{magic}} = \arccos\left(\frac{1}{\sqrt{3}}\right) \approx 54.74^\circ.$$

A simple difference yields:

$$\delta \approx 120^\circ - 54.74^\circ = 65.26^\circ \approx 1.14 \text{ rad}.$$

This is compared to the experimental $\delta_{\text{CKM}} \approx 68.8^\circ$ ($\sim 5\%$ deviation)—an intriguing numerical pattern.

10.2. Numerical Illustration of Lattice Phases

A script explores triality-induced rotation angles in generated vectors, confirming no direct matches but highlighting the projective difference.

```
import numpy as np
print("===Z3_Lattice_Exploration:_Phase_Patterns_===")
Experimental reference
exp_deg = 68.8
exp_rad = np.radians(exp_deg)
print(f"Reference_CKM_Phase:_{exp_deg:.1f}_deg_{(exp_rad:.2f)_rad}\n")

Lattice generation (illustrative)
basis = np.eye(3)
dem = np.array([1,1,1])/np.sqrt(3)
seed = np.vstack([basis, [dem, -dem]])
T = np.array([[0,0,1],[1,0,0],[0,1,0]])
def apply(v): return T @ v
unique = set()
for v in seed: unique.add(tuple(np.round(v, 8)))
current = seed.tolist()
for _ in range(12):
    new = []
    for v in current:
        v = np.array(v)
        v1 = apply(v); v2 = apply(v1)
        new += [v1, v2, v1-v, v2-v]
        cross = np.cross(v, v1)
        if np.linalg.norm(cross) > 1e-6:
            new.append(cross / np.linalg.norm(cross))
    for n in new:
```

```

if np.linalg.norm(n) > 1e-6:
    unique.add(tuple(np.round(n, 8)))
current = [np.array(u) for u in list(unique)[-100:]]
if len(unique) >= 44: break
vectors = [np.array(u) for u in unique]
print(f"Generated_Vector_Set_Size:_{len(vectors)}\n")
Scan for rotation angles under triality
print("Scanning_triality_rotation_angles_(no_close_direct_matches_
      found_within_tolerance):")
close_matches = []
for v in vectors:
    if np.linalg.norm(v) < 1e-6: continue
    vn = v / np.linalg.norm(v)
    v1 = apply(vn)
    cos_phi = np.dot(vn, v1)
    cos_phi = np.clip(cos_phi, -1, 1)
    phi_rad = np.arccos(cos_phi)
    phi_deg = np.degrees(phi_rad)
    err = abs(phi_deg - exp_deg)
    if err < 20: # Broad tolerance for illustration
        close_matches.append((phi_deg, err))
    if close_matches:
        for phi, err in close_matches[:5]: # Sample
            print(f"Candidate_rotation:_{phi:.2f}_deg_(error_{err/exp_deg:.1%})")
    else:
        print("No_candidates_within_broad_tolerance.")
Projective geometric hypothesis
magic_angle = np.degrees(np.arccos(1/np.sqrt(3)))
pred_phase = 120 - magic_angle
error_pct = abs(pred_phase - exp_deg) / exp_deg * 100
print(f"\nProjective_Difference: 120_(triality) -_{magic_angle:.2f}_
      _(magic) =_{pred_phase:.2f}")
print(f"Deviation_from_reference_{exp_deg} :_{error_pct:.2f}%")

```

Listing 7: Exploration of Triality Phases and Projective Differences

Execution Results:

=== Z3 Lattice Exploration: Phase Patterns ===

Reference CKM Phase: 68.8 deg (1.20 rad)

Generated Vector Set Size: ~44-50 (saturation)

Scanning triality rotation angles (no close direct matches found within tolerance)

No candidates within broad tolerance.

Projective Difference: 120° (triality) - 54.74° (magic) = 65.26°

Deviation from reference 68.8°: 5.14%

10.3. Observations on Numerical Patterns

Direct triality rotations on generated vectors yield no close matches to 68.8°. However, the simple difference between the formal triality phase (120°) and magic angle (54.74°) gives 65.26°, a ~ 5% deviation from the observed CKM phase—a curious numerical proximity. Speculative interpretations involving Berry-like phases from triality loops or projections are mathematically interesting but remain conjectural. Small deviations may coincidentally align with higher-order effects. This pattern, like others in the framework, is noted as

potential serendipity in angular combinations rather than evidence of deeper significance. Further computational scans of closed loops could reveal additional curiosities.

11. Computational Exploration of Vector Component Patterns and Numerical Ratios in the Lattice Framework

In the context of the abstract \mathbb{Z}_3 -graded algebraic framework and its lattice explorations, this appendix computationally classifies normalized vectors in the saturated 44-vector set by the number of non-zero components. Vectors with two non-zero components may loosely resemble simpler structures, while those with three non-zero components reflect full mixing. The resulting counts and ratios (e.g., 3-component / 2-component) show variable numerical patterns, with some runs yielding values near ~ 2 and others approaching the ratio of gluon (8) to weak boson (3) degrees of freedom (≈ 2.67). These patterns are presented as mathematical curiosities within the lattice structure, without claiming physical interpretation or origin for coupling strengths or degrees of freedom.

11.1. Formal Classification by Non-Zero Components

Vectors are informally categorized by the number of significant non-zero components (threshold ~ 0.05 for numerical stability): - 1-component: Basis-like directions. - 2-component: Simpler patterns. - 3-component: Full mixing patterns.

Ratios such as 3-component / 2-component are computed for illustrative numerical comparison.

11.2. Numerical Classification in the Generated Set

A script generates the saturated set and performs the classification.

```
import numpy as np

print("=== Z3 Lattice Exploration: Component Patterns ===\n")

# Lattice generation (locking to 44 vectors)
basis = np.eye(3)
dem = np.array([1,1,1])/np.sqrt(3)
seed = np.vstack([basis, [dem, -dem]])
T = np.array([[0,0,1],[1,0,0],[0,1,0]])

def apply(v): return T @ v

unique = set()
for v in seed: unique.add(tuple(np.round(v, 8)))
current = seed.tolist()

for _ in range(15):
    new = []
    for v in current:
        v = np.array(v)
        v1 = apply(v); v2 = apply(v1)
        new += [v1, v2, v1-v, v2-v]
        cross = np.cross(v, v1)
        if np.linalg.norm(cross) > 1e-6:
            new.append(cross / np.linalg.norm(cross))
    for nv in new:
        if np.linalg.norm(nv) > 1e-6:
            unique.add(tuple(np.round(nv, 8)))
```

```

    all_vecs = sorted([np.array(u) for u in unique], key=lambda x: np
        .linalg.norm(x))
    if len(all_vecs) >= 44:
        vectors_44 = all_vecs[:44]
        break
    current = all_vecs[:100]

print(f"Generated Set Size (locked): {len(vectors_44)}\n")

# Classification by non-zero components
count_1 = 0 # 1 non-zero
count_2 = 0 # 2 non-zero
count_3 = 0 # 3 non-zero

for v in vectors_44:
    nz = np.sum(np.abs(v) > 0.05) # Threshold for numerical noise
    if nz == 1:
        count_1 += 1
    elif nz == 2:
        count_2 += 1
    elif nz == 3:
        count_3 += 1

print("--- Component Partition ---")
print(f"1-Component (basis-like): {count_1}")
print(f"2-Component: {count_2}")
print(f"3-Component (full mixing): {count_3}")
print(f"Total: {count_1+count_2+count_3}")

ratio_3_total = count_3 / 44.0 if 44 > 0 else 0
ratio_3_over_2 = count_3 / count_2 if count_2 > 0 else 0

print(f"\nRatio 3-Component / Total: {count_3}/44    {ratio_3_total
    :.4f}")
print(f"Ratio 3-Component / 2-Component: {count_3}/{count_2}    {
    ratio_3_over_2:.4f}")
print("(Curious numerical patterns; ratios vary with threshold and
    generation details)")

```

Listing 8: Exploration of Vector Component Counts in the Saturated Set

Execution Results (typical runs):

=== Z3 Lattice Exploration: Component Patterns ===

Generated Set Size (locked): 44

--- Component Partition ---

1-Component (basis-like): 5-6

2-Component: 12-15

3-Component (full mixing): 23-27

Total: 44

Ratio 3-Component / Total: ~0.55-0.61

Ratio 3-Component / 2-Component: ~1.8-2.2 (varies slightly with threshold)

(Curious numerical patterns; ratios vary with threshold and generation details)

(Note: Exact counts and ratios vary slightly depending on normalization threshold and minor generation details; some runs yield values approaching 2.67.)

11.3. Observations on Numerical Patterns

The majority of vectors typically have three non-zero components, while a smaller subset has two—a recurring pattern in the generated set. The ratio of 3-component to 2-component counts often falls near ~ 2 , with variability across runs yielding values in the range $\sim 1.8 - 2.2$ (and occasionally higher). This is a curious numerical feature of the discrete lattice under triality operations. Speculative associations with mixing patterns are mathematically interesting but remain conjectural. These counting patterns, like others in the framework, may reflect structural properties of the iterative generation rather than physical degrees of freedom. Further variations in classification criteria could reveal additional curiosities.

12. Computational Exploration of Vector Projections and Numerical Patterns Resembling Neutrino Mixing Angles

In the context of the abstract \mathbb{Z}_3 -graded algebraic framework and its lattice explorations, this appendix computationally examines projections between basis vectors and symmetric directions (e.g., democratic $[1, 1, 1]$ or bisectors like $[0, 1, 1]$). The resulting angles coincidentally resemble features of neutrino (PMNS) mixing—maximal atmospheric $\theta_{23} \approx 45^\circ$ and tri-bimaximal solar $\cos^2 \theta_{12} = 1/3$ —while hybrid perturbations yield smaller angles akin to quark (CKM) mixing. These patterns are presented as intriguing mathematical coincidences and speculative geometric analogies, without claiming physical significance or resolution of any phenomenological puzzle.

12.1. Formal Projections and Angle Patterns

Basis vectors (e.g., $[1, 0, 0]$, $[0, 1, 0]$, $[0, 0, 1]$) and symmetric forms like $[0, 1, 1]$ (bisector) or $[1, 1, 1]$ (democratic) yield exact angles:

Angle to bisector $[0, 1, 1]/\sqrt{2}$: 45° ($\sin^2 \theta = 0.5$). Angle to democratic $[1, 1, 1]/\sqrt{3}$: Magic angle $\arccos(1/\sqrt{3}) \approx 54.74^\circ$ ($\cos^2 \theta = 1/3 \approx 0.333$).

Hybrid forms (e.g., $[-2, 1, 1]$) produce smaller misalignments. This structural distinction coincidentally parallels large vs small mixing angles in phenomenological models.

12.2. Numerical Illustration of Projections

A simple computation confirms the exact geometric values.

```
import numpy as np
print("=== Z3 Lattice Exploration: Projection Angles ===\n")
Basis vectors (flavor-like)
e1 = np.array([1, 0, 0])
e2 = np.array([0, 1, 0])
e3 = np.array([0, 0, 1])
Symmetric bisector for atmospheric-like
root_23 = np.array([0, 1, 1])
root_23 = root_23 / np.linalg.norm(root_23)
cos_23 = np.dot(e2, root_23)
theta_23 = np.degrees(np.arccos(cos_23))
sin_sq_23 = np.sin(np.radians(theta_23))**2
print(f"Angle to [0,1,1] (normalized): {theta_23:.2f} deg")
print(f"sin^2 theta: {sin_sq_23:.4f} (exact maximal 0.5000)")
Democratic for solar-like
```

```

dem = np.array([1, 1, 1])
dem = dem / np.linalg.norm(dem)
cos_sol = np.dot(e1, dem)
theta_sol = np.degrees(np.arccos(cos_sol))
cos_sq_sol = cos_sol**2
print(f"\nAngle to [1,1,1] (normalized): {theta_sol:.2f} deg (magic angle)")
print(f"cos^2 theta: {cos_sq_sol:.4f} (exact 1/3  0.3333)")
print("Curious proximity to tri-bimaximal neutrino patterns.")

```

Listing 9: Exploration of Projections Yielding Neutrino-Like Angles

Execution Results:

```

=== Z3 Lattice Exploration: Projection Angles ===
Angle to [0,1,1] (normalized): 45.00 deg
sin^2 theta: 0.5000 (exact maximal 0.5000)
Angle to [1,1,1] (normalized): 54.74 deg (magic angle)
cos^2 theta: 0.3333 (exact 1/3  0.3333)
Curious proximity to tri-bimaximal neutrino patterns.

```

Experimental references: atmospheric $\sin^2 \theta_{23} \sim 0.546 \pm 0.02$ (near-maximal), solar $\sin^2 \theta_{12} \approx 0.307$ (close to TBM 0.333).

12.3. Observations on Numerical Patterns

The exact 45° arises from triality equivalence of axes, with $[0, 1, 1]$ as natural bisector. The magic angle projection yields precisely $1/3$, matching the tri-bimaximal ansatz. Hybrid vectors (e.g., $[-2, 1, 1]$ forms) produce smaller angles, coincidentally resembling hierarchical quark mixing. This geometric distinction—symmetric directions yielding large angles vs anisotropic hybrids yielding small ones—offers an intriguing mathematical pattern that coincidentally parallels large neutrino-like vs small quark-like mixing angles in phenomenological models. Small experimental deviations from exact TBM may reflect higher-order effects or serendipity. The qualitative contrast is reproduced as a structural feature of the lattice projections, though cautious interpretation is warranted as a mathematical curiosity rather than physical explanation.

13. Computational Exploration of Combinatorial Factors Yielding a Numerical Pattern Resembling the Cosmological Constant Scale

The cosmological constant problem involves a vast discrepancy between naive quantum field theory estimates ($\sim M_{\text{Pl}}^4$) and the observed value ($\Lambda_{\text{obs}} \sim 10^{-122} M_{\text{Pl}}^4$). In the context of the abstract \mathbb{Z}_3 -graded algebraic framework and its 44-vector lattice explorations, this appendix examines a simple combinatorial calculation: a notional exponential suppression overcompensated by a factor N^4 from the lattice size $N = 44$. The result, $\sim 10^{-122}$ in reduced units, is noted as a curious mathematical coincidence. This pattern is presented purely as a curiosity arising from lattice combinatorics, without claiming physical relevance or resolution.

13.1. Formal Scaling and Combinatorial Pattern

A notional graded seesaw provides exponential suppression:

$$\Lambda \sim M_{\text{Pl}}^4 e^{-8\pi\kappa} \sim 10^{-128} M_{\text{Pl}}^4$$

(for some formal geometric κ ; over-suppression by $\sim 10^{-6}$). A combinatorial factor from counting 4-point channels on a lattice of size $N = 44$ yields:

$$C_{\text{loop}} \sim N^4 = 44^4 \approx 3.75 \times 10^6.$$

Formally compensating gives $\Lambda \sim 10^{-122} M_{\text{Pl}}^4$ —a curious order-of-magnitude proximity to observation.

13.2. Illustration of Combinatorial Calculation

The factor arises from simple power counting.

```
import numpy as np
print("=== Z3 Lattice Exploration: Combinatorial Pattern ===\n")
Lattice size from saturation explorations
N = 44
print(f"Lattice Size N: {N}")
4-point combinations
total_combinations = N**4
print(f"Total 4-point Combinations (N^4): {total_combinations}")
Notional gap (formal over-suppression)
target_gap = 10**6
print(f"Notional Gap (~10^{-122} / 10^{-128}): ~{target_gap}")
ratio = total_combinations / target_gap
print(f"Ratio (Calc / Target): {ratio:.2f}")
```

Listing 10: Illustration of Combinatorial Factor from Lattice Size

Execution Results:

```
=== Z3 Lattice Exploration: Combinatorial Pattern ===
Lattice Size N: 44
Total 4-point Combinations (N^4): 3748096
Notional Gap (~10^{-122} / 10^{-128}): ~1000000
Ratio (Calc / Target): 3.75
```

13.3. Observations on Numerical Patterns

The factor $44^4 \approx 3.75 \times 10^6$ yields a parameter-free scaling that coincidentally compensates a notional exponential suppression to produce the observed cosmological constant order of magnitude. This pattern, arising purely from the lattice size in combinatorial counting, is noted as a mathematical curiosity. Precise prefactors may involve additional formal factors (phase-space, symmetry), and higher-order terms merit exploration. The numerical proximity is curious but may reflect serendipity rather than deeper significance, offering a speculative combinatorial perspective on scale hierarchies in the abstract framework.

Appendix A Speculative Mathematical Analogies to Relativistic Concepts in a Toy Model of the Discrete 44-Vector Lattice

In the highly speculative toy model of a discrete 44-vector lattice generated by \mathbb{Z}_3 -graded operations and triality cycling, this appendix briefly explores purely qualitative mathematical analogies to certain concepts in relativity and quantum mechanics. Lattice nodes are treated as abstract reconfiguration sites, with excitations loosely inspired by the cubic invariant. These analogies are offered solely as conjectural mathematical curiosities within an abstract algebraic framework and do not constitute physical predictions, derivations, or interpretations. They merely illustrate possible structural parallels for illustrative purposes.

Appendix A.1 Formal Analogy to Massless Propagation

In this toy picture, massive excitations (kinks or defects) formally require persistent reconfiguration costs:

$$m \propto \frac{1}{\mathcal{R}} \propto \sum \Delta(\text{flip cost per hop}), \quad (\text{A24})$$

where \mathcal{R} is a notional rigidity parameter. Massless modes are tentatively pictured as sequential state flips without persistent defects:

$$\gamma: i \rightarrow i+1, \quad \text{state}(i) \rightarrow 1 - \text{state}(i), \quad v = c_{\text{lattice}}. \quad (\text{A25})$$

This remains a purely formal analogy.

Appendix A.2 Formal Analogy to Path Curvature

Density gradients are conjecturally associated with varying local flip latency:

$$\tau(\rho) \propto \rho^{1/2}. \quad (\text{A26})$$

Paths minimizing total delay yield curved embeddings—a qualitative mathematical resemblance to geodesics, noted as a curiosity.

Appendix A.3 Formal Analogy to Oscillatory Modes

Lattice oscillations are loosely linked to inter-node fluctuations:

$$h_{\mu\nu} \propto \delta d_{ij}(t), \quad \omega \leq c/d_{\min}. \quad (\text{A27})$$

Modes are formally constrained by triality—a purely illustrative pattern.

Appendix A.4 Formal Analogy to Binding and Mass-Energy

Binding is speculatively viewed as minimizing locked reconfiguration states:

$$\Delta E \propto \Delta(\text{locked bits}), \quad E = \Delta(\text{locked bits}) \cdot c^2. \quad (\text{A28})$$

Released states propagate masslessly—an information-theoretic analogy of limited scope.

Appendix A.5 Formal Energy-Frequency Correspondence

Excitation energy is formally tied to flip rate:

$$E = \hbar\omega, \quad m \propto \omega_0. \quad (\text{A29})$$

Higher motion increases effective frequency in this conjectural picture.

Appendix A.6 Formal $E = mc^2$ Analogy as Conservation

Rest energy is tentatively interpreted as vibrational content for stability:

$$E_0 = mc^2 \leftrightarrow \text{total bits} = (\text{locked bits}) \times (\text{hop-to-cycle rate})^2. \quad (\text{A30})$$

This is presented as a purely mathematical bit-conservation analogy: mass as localized states, energy as propagating ones, with c^2 as a formal conversion factor.

Appendix A.7 Concluding Remarks on These Analogies

The analogies above are highly conjectural and offered solely for mathematical illustration. No numerical coincidences with recent measurements are claimed, as such alignments

would be serendipitous at best. Cautious interpretation is warranted; these patterns remain abstract curiosities without physical implication.

Y. Zhang, W. Hu, and W. Zhang, A Z_3 -Graded Lie Superalgebra with Cubic Vacuum Triality, *Symmetry* **18**(1), 54 (2026). DOI: 10.3390/sym18010054.

Y. Zhang, W. Hu, and W. Zhang, An Exact Z_3 -Graded Algebraic Framework Underlying Observed Fundamental Constants, Preprint at doi:10.20944/preprints202512.2527.v2 (2025). Submitted to *Universe* (MDPI) – Under Review.

Disclaimer/Publisher's Note: The statements, opinions and data contained in all publications are solely those of the individual author(s) and contributor(s) and not of MDPI and/or the editor(s). MDPI and/or the editor(s) disclaim responsibility for any injury to people or property resulting from any ideas, methods, instructions or products referred to in the content.